· Original article ·

Electroacupuncture intervention on choroidal blood perfusion and the PI3K/Akt/mTOR-HIF-1α signaling pathway in myopic guinea pigs

Qin Han[1], *Zhao Yong*[1], *Liu Meng*[1], *Wang Yan*[1], *Zhou Shun*[2], *Ma Dingcheng*[2], *Gao Yunxian*[1]

引用:秦汉,赵勇,浏梦,等. 电针干预对近视豚鼠脉络膜血流灌注及 PI3K/Akt/mTOR-HIF-1α 信号通路的影响. 国际眼科杂志, 2026,26(6):923-930.

Foundation items: General Program of the Natural Science Foundation of the Department of Science and Technology of Xinjiang Uygur Autonomous Region (No.2022D01C551); Key Hospital-Level Research Project of the Fourth Affiliated Hospital of Xinjiang Medical University (No.ZYY2022ZD4)

[1]Department of Ophthalmology, the Fourth Affiliated Hospital of Xinjiang Medical University, Urumqi 830000, Xinjiang Uygur Autonomous Region, China; [2]Fourth Clinical Medical College, Xinjiang Medical University, Urumqi 830000, Xinjiang Uygur Autonomous Region, China

Correspondence to: Gao Yunxian. Department of Ophthalmology, the Fourth Affiliated Hospital of Xinjiang Medical University, Urumqi 830000, Xinjiang Uygur Autonomous Region, China. gaoyx6362@163.com

Received: 2025-08-01 Accepted: 2026-03-12

电针干预对近视豚鼠脉络膜血流灌注及 PI3K/Akt/mTOR-HIF-1α 信号通路的影响

秦 汉[1],赵 勇[1],浏 梦[1],王 雁[1],周 顺[2],马鼎程[2],高云仙[1]

基金项目:新疆维吾尔自治区科学技术厅自然科学基金面上项目(No.2022D01C551);新疆医科大学第四附属医院院级课题重点项目(No.ZYY2022ZD4)

作者单位:[1](830000)中国新疆维吾尔自治区乌鲁木齐市,新疆医科大学第四附属医院眼科;[2](830000)中国新疆维吾尔自治区乌鲁木齐市,新疆医科大学第四临床医学院

作者简介:秦汉,毕业于湖南中医药大学,硕士,副主任医师,研究方向:屈光不正、斜弱视的中西医结合防治。

通讯作者:高云仙,毕业于新疆医科大学,硕士,主任医师,眼科主任,研究方向:屈光不正的基础、临床及流行病学. gaoyx6362@163.com

摘要

目的:研究电针(EA)对形觉剥夺诱导近视(FDM)豚鼠脉络膜血流、PI3K/Akt/mTOR-HIF-1α 信号通路以及眼部生物学参数的影响。

方法:将豚鼠随机分为 4 组:空白对照组、FDM 组(通过形觉剥夺模拟近视发展)、FDM+电针(FDM+EA)组(形觉剥夺并接受电针刺激)、FDM+假穴(FDM+sham)组(形觉剥夺并接受电针刺激)。FDM+EA 组在太阳穴(EX-HN5)穴位进行电针治疗,FDM+sham 组在假穴点进行电针治疗。测量指标包括屈光度、眼轴轴长(AL)、角膜曲率、玻璃体直径、脉络膜厚度、脉络膜层的血管密度。此外,还检测了巩膜中 PI3K、Akt、mTOR、HIF-1α mRNA 的表达水平。

结果:每组均纳入 8 只豚鼠,治疗 4 wk 后,FDM+EA 组的屈光度较 FDM 组显著降低($P<0.001$),FDM+EA 组脉络膜血管密度较 FDM 组显著增加($P<0.001$),FDM+EA 组中 PI3K、Akt、mTOR 及 HIF-1α mRNA 表达水平较 FDM 组显著降低($P<0.001$)。

结论:电针疗法可提高脉络膜血管密度,抑制 PI3K/Akt/mTOR-HIF-1α 信号通路的表达,有效改善巩膜缺氧状态,降低近视豚鼠的屈光度,对控制近视进展具有积极作用。

关键词:近视;脉络膜血流灌注;PI3K/Akt/mTOR-HIF-1α 信号通路;电针疗法

Abstract

• AIM: To study the effects of electroacupuncture (EA) on choroidal blood flow, the phosphatidylinositol 3-kinase (PI3K)/protein kinase B (Akt)/mammalian target of rapamycin (mTOR)-hypoxia-inducible factor 1-alpha (HIF-1α) signaling pathway, and ocular biological parameters in form deprivation myopia (FDM)-induced guinea pigs.

• METHODS: The guinea pigs were randomly divided into four groups: blank control group; FDM group (subjected to form deprivation to simulate myopia development); FDM+EA group (subjected to form deprivation and treated with EA stimulation); FDM+sham acupuncture group (subjected to form deprivation and given EA stimulation). EA treatments were performed at the Taiyang (EX-HN5) acupoint for the FDM+EA group and at sham acupoints in the FDM+sham group. Measurements included refractive error, axial length (AL), corneal curvature, vitreous diameter, choroidal thickness, and vascular density of the choroid layer. Additionally, the expression levels of PI3K, Akt, mTOR, and HIF-1α mRNA in the sclera were detected.

• RESULTS: Eight animals were included in each group. After 4 wk of treatment, the refractive error of the FDM+EA group was significantly reduced compared to the FDM group ($P<0.001$). The vascular density of the choroid in the FDM+EA group was significantly increased compared

to the FDM group ($P<0.001$). The expression levels of PI3K, Akt, mTOR, and HIF-1α mRNA in the FDM+EA group were significantly reduced compared to the FDM group ($P<0.001$).

• CONCLUSION: EA can improve the vascular density of choroid, antagonize the expression of PI3K/Akt/mTOR-HIF-1α signaling pathway, effectively improve scleral hypoxia, reduce the diopter of myopic guinea pigs, and play a role in controlling the progression of myopia.

• KEYWORDS: myopia; choroidal blood perfusion; PI3K/Akt/mTOR-HIF-1α signaling pathway; electroacupuncture
DOI:10.3980/j.issn.1672-5123.2026.6.01

Citation: Qin H, Zhao Y, Liu M, et al. Electroacupuncture intervention on choroidal blood perfusion and the PI3K/Akt/mTOR-HIF-1α signaling pathway in myopic guinea pigs. Guoji Yanke Zazhi (Int Eye Sci), 2026,26(6):923-930.

INTRODUCTION

Myopia refers to a refractive error that causes light to focus in front of the retina, resulting in clear near vision but blurred distancevision[1]. The findings revealed a gradual increase in pooled prevalence of myopia, ranging from 24.32% to 35.81%, observed from 1990 to 2023, and projections indicate that this prevalence is expected to reach 36.59% in 2040 and 39.80% in 2050. Notably, individuals residing in East Asia (35.22%) or in urban areas (28.55%), female gender (33.57%), adolescents (47.00%), and high school students (45.71%) exhibit a higher proportion of myopia prevalence.The global prevalence of childhood myopia is substantial, affecting approximately one-third of children and adolescents, with notable variations in prevalence across different demographic groups. It is anticipated that the global incidence of myopia will exceed 740 million cases by 2050[2]. The prevalence of myopia among adolescent students in Yili, Xinjiang Uygur Autonomous Region, China was 26.28%, and gradually increased with age. It is necessary to strengthen the awareness of myopia prevention and control among primary and secondary school students and reduce the myopia rate[3].

Progression of myopia to high myopia can lead to a series of retinal pathologies, severely impairing vision, reducing quality of life, and consuming substantial medical resources[4-5]. Consequently, preventing myopia has become a global health consensus[6].

Current treatments for myopia include cycloplegia, corrective lenses, orthokeratology, laser refractive surgery, and implantable collamer lenses (ICL)[7]. However, these approaches have shown limited efficacy in myopia prevention and control in China, highlighting an urgent issue in the nation's healthcare system. Over years of clinical practice, our department has developed a technique for treating myopia through acupuncture, which has demonstrated promising clinical efficacy, though its specific mechanism remains to be studied.

Our preliminary research has shown that acupuncture treatment for adolescent myopia can reduce spherical equivalent refraction, shorten the anterior-posterior diameter of the lens, and decrease ciliary body thickness, with high safety[8]. Additionally, we found that acupuncture inhibits ocular elongation in myopic rats, promotes transforming growth factor beta 2 (TGF-β2) secretion, reduces the expression of matrix metalloproteinase 2 (MMP2) mRNA and protein in scleral tissues, and increases the expression of Collagen I mRNA and protein, thus antagonizing scleral remodeling and inhibiting myopia progression[9]. However, a 2020 Cochrane review concluded that the evidence for acupuncture's efficacy in myopia management was of very low certainty due to risk of bias and heterogeneity among studies[10]. However, there is currently a lack of deeper research into the mechanisms underlying acupuncture treatment for myopia. Based on this, we hypothesize that acupuncture may influence the process of scleral remodeling by regulating scleral hypoxia.

This study aims to investigate the effects of electroacupuncture (EA) intervention on form deprivation myopia (FDM) in guinea pigs by observing changes in ocular biological measurements [refractive error, axial length (AL), vitreous diameter, corneal curvature], as well as its impact on choroidal thickness and choroidal vascular density. We aim to explore the role of EA in the scleral remodeling process in myopia.

MATERIALS AND METHODS

Ethical Approval All experimental protocols and animal ethics were approved and conducted in accordance with the Animal Ethics Committee of Xinjiang Medical University and approved by the Ethics Committee of the Traditional Chinese Medicine Hospital of Xinjiang Uygur Autonomous Region, with approval number 2023XE0132. This study was reported in accordance with the ARRIVE 2.0 guidelines[11] and conducted in accordance with the ARVO Statement for the Use of Animals in Ophthalmic and Vision Research.

Animals Three-week-old male tricolor guinea pigs (150-200 g) were provided by Shaanxi Junxing Biotechnology Co., Ltd. (SCXK Shaanxi 2022-01). The guinea pigs were housed under a 12-hour light/12-hour dark cycle, with room temperature maintained at 25 ℃. They had free access to water and food.

Grouping The guinea pigs were randomly divided into four groups, with 8 animals in each group. 1) Blank control group: no interventions; 2) FDM group: subjected to form deprivation to simulate myopia development; 3) FDM+sham acupuncture group: subjected to form deprivation and given EA stimulation at sham acupoints; 4) FDM+EA group: subjected to form deprivation and given EA stimulation 0.5 cm above the temporal acupoint (EX-HN5 Taiyang).

Methods The FDM model was established using a white latex balloon head cap(≥80% transmission) that covered the right eye (experimental eye) of the guinea pigs while leaving the left eye (control eye) uncovered. This setup induced

monocular form deprivation, while the nose and both ears were exposed to ensure normal feeding. The head cap was inspected and cleaned daily to ensure light transparency. Guinea pigs in the blank control group were not subjected to any interventions. Diopter −1.50 D is the lowest threshold for inclusion in the successful group of FDM modeling.

Electroacupuncture stimulation method Guinea pigs in the FDM+EA group received EA stimulation bilaterally at the temporal acupoints (EX-HN5) every other day for 20 min. The stimulation parameters were as follows: biphasic square wave, 0.1 ms pulse width, frequency of 2 Hz, pulse duration of 0.1 s, and intensity of 2.0 mA, skin impedance was verified and maintained below a standard threshold (<5 kΩ) before each session. Interventions for all groups were conducted continuously for 4 wk. Guinea pigs in the FDM and blank control groups received no treatment.

Ocular biological measurements Measurements of refractive error, AL, vitreous diameter, and corneal curvature were taken before modeling, after modeling, and after EA intervention.

Refractive error measurement The refractive error of guinea pigs was measured using a small animal infrared eccentric photorefractor (SriaTech, Germany; model: photorefractor). Measurements were taken before modeling, 4 wk after modeling, and 4 wk after treatment. Prior to measurement, compound tropicamide eye drops were administered for mydriasis, with one drop every 5 min for a total of four applications. Refractive error was measured 30 min after the final application using the infrared photorefractor.

Axial length and vitreous diameter measurement AL and vitreous diameter were measured using an A-mode ultrasound device for animals (Xuzhou Kaixin Electronic Equipment Co., Ltd.; model: OD1-A). The A-mode ultrasound probe was positioned perpendicularly to the corneal apex during measurement.

Corneal curvature measurement Corneal curvature was measured using a small animal keratometer (SriaTech, Germany; model: Keratometer). All measurements were performed by the same trained technician to ensure consistency.

Changes in Choroidal Thickness and Vascular Density Before and After EA Using the BM-400K macular optical coherence tomography angiography (OCTA) system (Tuopai Medical Technology Co., Ltd., Beijing, China), optical coherence tomography (OCT) was employed to scan the retina and choroid. The macular OCTA mode was selected with a scan length of 12 mm×12 mm and a depth of field of 3 mm. OCTA scanning was performed until the program completed, yielding a macular OCTA report. The choroidal blood flow was quantified by selecting the flow quantification mode (3 mm×3 mm). Choroidal thickness was quantified by selecting the thickness display report. All operations were conducted by the same experienced technician. Re-scan and re-analyze a subset of eyes ($n=10$ across groups) after a 24-hour interval and calculate the intraclass correlation coefficient (ICC). An ICC ≥0.85 is generally considered excellent.

qRT-PCR for Detecting mRNA Changes in the PI3K/Akt/mTOR-HIF-1α Signaling Pathway

RNA extraction procedure Tissues were ground into powder under liquid nitrogen. Approximately 50 mg of tissue was placed into a centrifuge tube containing 1 mL of TRIzol reagent and mixed thoroughly. The mixture was incubated at room temperature for at least 15 min, followed by the addition of 200 μL of chloroform. The mixture was shaken and incubated at room temperature for 5 min. It was then centrifuged at 12 000 rpm at 4 ℃ for 15 min. The supernatant was transferred to a new centrifuge tube, and an equal volume of isopropanol was added and mixed. The mixture was stored at −20 ℃ for 60 min, then centrifuged again at 12 000 rpm at 4 ℃ for 15 min. The supernatant was carefully discarded, and the pellet was washed with 75% ethanol. This step was repeated once. The sample was air-dried after centrifugation and dissolved in RNase-free water. RNA concentration was determined using a nucleic acid protein quantification instrument, and RNA integrity was verified by agarose gel electrophoresis. RNA was reverse transcribed for subsequent experiments.

First-Strand cDNA Synthesis

Reaction system was configured according to Table 1 The mixture was gently mixed and subjected to the following reactions: 37 ℃ for 15 min, 60 ℃ for 10 min, and 95 ℃ for 3 min to inactivate the enzyme, completing the reverse transcription. The resulting complementary DNA (cDNA) cDNA was stored at −80 ℃ for subsequent quantitative real-time polymerase chain reaction (qRT-PCR). The cDNA samples were diluted at a 1∶1 ratio with RNase-free water for the qRT-PCR reactions. Primer information for fluorescence quantification is shown in Table 2.

Primers were designed based on the gene sequences. PCR reaction conditions were as follows: 95 ℃ for 30 s → 95 ℃ for 5 s → 60 ℃ for 31 s, repeated for 40 cycles. After the reaction, samples were stored at −20 ℃. Each batch of samples underwent simultaneous amplification of glyceraldehyde-3-phosphate dehydrogenase (GAPDH, as an internal reference) and the target genes. The ΔCt values of phosphatidylinositol 3-kinase (PI3K)/protein kinase B (Akt)/mammalian target of rapamycin (mTOR), and hypoxia-inducible factor 1-alpha (HIF-1α) in guinea pig scleral tissues were calculated, and the relative expression levels of the target genes were analyzed using the $2^{-\Delta\Delta Ct}$ method.

Table 1 First-strand cDNA synthesis configuration

Component	Volume
Total RNA	Quantify to 1000 ng
5X All-In-One RTMasterMix	4 μL
RNase-free water	Up to 20 μL

cDNA: Complementary DNA.

Table 2 Fluorescence quantitative mRNA primer information

Primer name	Sequence (5' to 3')	Product size
gp-PI3K-F	TGCATCAGTGGCTCAAAGAC	117 bp
gp-PI3K-R	GGTCACCAATTCCCAAAATG	
gp-AKT1-F	ACCTCATGCTGGACAAGGAC	233 bp
gp-AKT1-R	CTTCTCGTGGTCCTGGTTGT	
gp-mTOR-F	CTGAAATGCAGGAACAGCAA	208 bp
gp-mTOR-R	CTGACCTCACAGCCACAGAA	
gp-HIF-1α-F	TGGAGATGTTGGCACCCTA	134 bp
gp-HIF-1α-R	TTGAGTCTGCTGGAATGCTG	
gp-GAPDH-F	TTCGTGATGGGCGTGAATCA	156 bp
gp-GAPDH-R	AGTGATGGCATGGACTGTGG	

PI3K: Phosphatidylinositol 3-kinase; AKT1: AKT serine/threonine kinase 1; mTOR: Mammalian target of rapamycin; HIF-1α: Hypoxia-inducible factor 1-alpha; GAPDH: Glyceraldehyde-3-phosphate dehydrogenase.

Statistical Analysis SPSS22.0 was used for statistical analysis of the data. Kolmogorov-Smirnov test was used to test the normality of the data. The normality was described by mean and standard deviation. The difference between the two groups was compared by *t* test, and the comparison between multiple groups was analyzed by analysis of variance. Further pairwise comparison was performed using least significant difference (LSD) test. Non-normality was described by median and quartile. Mann-Whitney *U* test was used to compare the differences between the two groups. Kruskal-Wallis H test was used for comparison between multiple groups, and Steel-Dwass test was used for further pairwise comparison. The overall selection test level of the study was 0.05 on both sides.

RESULTS

Changes Before and After EA Treatment in Myopic Guinea Pigs

Axial length No significant differences were observed among the four groups before modeling ($P=0.175$). Compared with baseline (before modeling), the AL in the FDM group, FDM+EA group, and FDM+sham acupuncture group significantly increased after 4 wk of modeling ($P<0.001$). After 4 wk of treatment, no significant difference in AL growth was observed between the FDM+EA and FDM+sham acupuncture groups compared to the FDM group ($P=0.380$; Table 3).

Vitreous diameter No significant differences were observed among the four groups before modeling ($P=0.319$). Compared with baseline, the vitreous diameter in the FDM group, FDM+EA group, and FDM+sham acupuncture group significantly increased after 4 wk of modeling ($P<0.001$). After 4 wk of treatment, no significant difference in vitreous diameter growth was observed between the FDM+EA and FDM+sham acupuncture groups compared to the FDM group ($P=0.125$; Table 3).

Refractive error No significant differences were observed among the four groups before modeling ($P=0.186$). Compared with baseline, the myopic refractive error in the FDM group, FDM+EA group, and FDM+sham acupuncture group significantly increased after 4 wk of modeling ($P<0.001$), indicating statistical significance and confirming the successful establishment of the myopic guinea pig model. After 4 wk of treatment, the myopic refractive error significantly decreased in the FDM+EA group compared to the FDM group ($P<0.001$). The data of refractive error did not satisfy the normal distribution, and the generalized estimation equation was used to analyze the difference between different groups at each time point. The statistical analysis of the results of each group is detailed in Table 3.

Corneal curvature No significant differences were observed among the four groups ($P=0.434$). Compared with baseline, the corneal curvature in the FDM group, FDM+EA group, and FDM+sham acupuncture group significantly decreased after 4 wk of modeling ($P<0.001$). After 4 wk of treatment, no significant differences in corneal curvature were observed between the FDM+EA and FDM+sham acupuncture groups compared to the FDM group ($P=0.762$; Table 3).

Choroidal vascular density No significant differences were observed among the four groups before modeling ($P=0.305$). Compared with baseline, the choroidal vascular density in the FDM group, FDM+EA group, and FDM+sham acupuncture group significantly decreased after 4 wk of modeling ($P<0.001$). After 4 wk of treatment, the choroidal vascular density in the FDM+EA group significantly increased compared to the FDM group ($P<0.001$; Figures 1-4).

Choroidal thickness No significant differences were observed among the four groups before modeling ($P=0.207$). Compared with baseline, the choroidal thickness in the FDM group, FDM+EA group, and FDM+sham acupuncture group significantly decreased after 4 wk of modeling ($P<0.001$). After 4 wk of treatment, no significant differences in choroidal thickness were observed between the FDM+EA and FDM+sham acupuncture groups compared to the FDM group ($P=0.057$; Figures 1-4).

EA on PI3K/Akt/mTOR-HIF-1α Signaling Pathway mRNA Before and After Treatment After 4 wk of EA treatment, compared with the control group, the mRNA levels of PI3K, Akt, mTOR, and HIF-1α in the FDM group were significantly elevated ($P<0.001$). Compared with the FDM group, the mRNA levels of PI3K, Akt, mTOR, and HIF-1α in the FDM+EA group were significantly decreased ($P<0.001$; Table 4).

DISCUSSION

The experimental results show that after successful myopia modeling, the myopic refractive error in the FDM group, FDM+EA group, and FDM+sham acupuncture group significantly increased, it may indicate the successful establishment of the myopia guinea pig model and demonstrating

Table 3 Analysis of parameters at different times and in different groups $\bar{x}\pm s$

Parameters	Control group	FDM group	FDM+EA group	FDM+sham group	F	P
Axial length (mm)						
Before modeling	8.35±0.23	8.33±0.25	8.32±0.25	8.35±0.22	$F_{interclass}=2.519$	$P_{interclass}=0.175$
4 wk after modeling	8.37±0.25	8.66±0.34	8.53±0.27	8.6±0.33	$F_{intra-class}=54.626$	$P_{intra-class}<0.001$
4 wk after treatment	8.32±0.25	8.69±0.32	8.62±0.29	8.55±0.26	$F_{Interaction}=1.080$	$P_{Interaction}=0.380$
Vitreous diameter (mm)						
Before modeling	4.96±0.16	4.94±0.18	4.96±0.14	4.96±0.14	$F_{interclass}=3.747$	$P_{interclass}=0.319$
4 wk after modeling	4.94±0.17	5.24±0.18	5.15±0.16	5.17±0.22	$F_{intra-class}=71.960$	$P_{intra-class}<0.001$
4 wk after treatment	4.95±0.21	5.28±0.25	5.20±0.23	5.10±0.15	$F_{Interaction}=1.716$	$P_{Interaction}=0.125$
Refractive error (D)						
Before modeling	1.25 (0.75, 2.50)	1.00 (0.25, 2.72)	1.25 (0.75, 2.00)	1.25 (0.50, 2.00)	$\chi^2_{interclass}=2.675$	$P_{interclass}=0.186$
4 wk after modeling	1.20 (1.00, 2.25)	−3.37 (−5.18, −2.61)	−1.50 (−1.65, −1.14)	−1.44 (−2.20, −1.00)	$\chi^2_{intra-class}=32.471$	$P_{intra-class}<0.001$
4 wk after treatment	1.25 (1.00, 2.00)	−2.93 (−4.35, −2.19)	−0.70 (−0.95, 0)	−1.53 (−1.95, −0.90)	$\chi^2_{Interaction}=45.219$	$P_{Interaction}<0.001$
Corneal curvature (D)						
Before modeling	4.04±0.15	4.05±0.07	4.06±0.11	4.01±0.06	$F_{interclass}=0.922$	$P_{interclass}=0.434$
4 wk after modeling	4.02±0.21	2.01±0.20	2.14±0.30	2.07±0.32	$F_{intra-class}=4336.549$	$P_{intra-class}<0.001$
4 wk after treatment	4.06±0.16	1.96±0.04	1.97±0.30	1.98±0.13	$F_{Interaction}=0.559$	$P_{Interaction}=0.762$
Choroidal vascular density (%)						
Before modeling	52.14±2.41	52.29±2.02	52.95±2.88	52.60±2.67	$F_{interclass}=9.256$	$P_{interclass}=0.305$
4 wk after modeling	52.64±2.33	48.59±2.98	45.63±3.17	49.13±3.11	$F_{intra-class}=61.462$	$P_{intra-class}<0.001$
4 wk after treatment	52.96±1.79	48.24±2.49	53.21±1.69	49.53±3.31	$F_{Interaction}=20.239$	$P_{Interaction}<0.001$
Choroidal thickness (μm)						
Before modeling	68.11±8.04	69.41±6.34	67.89±10.02	67.27±14.37	$F_{interclass}=1.557$	$P_{interclass}=0.207$
4 wk after modeling	68.61±6.38	61.18±7.46	60.00±8.07	56.33±12.23	$F_{intra-class}=60.175$	$P_{intra-class}<0.001$
4 wk after treatment	68.32±8.55	55.82±7.56	53.05±8.36	53.27±12.95	$F_{Interaction}=1.885$	$P_{Interaction}=0.057$

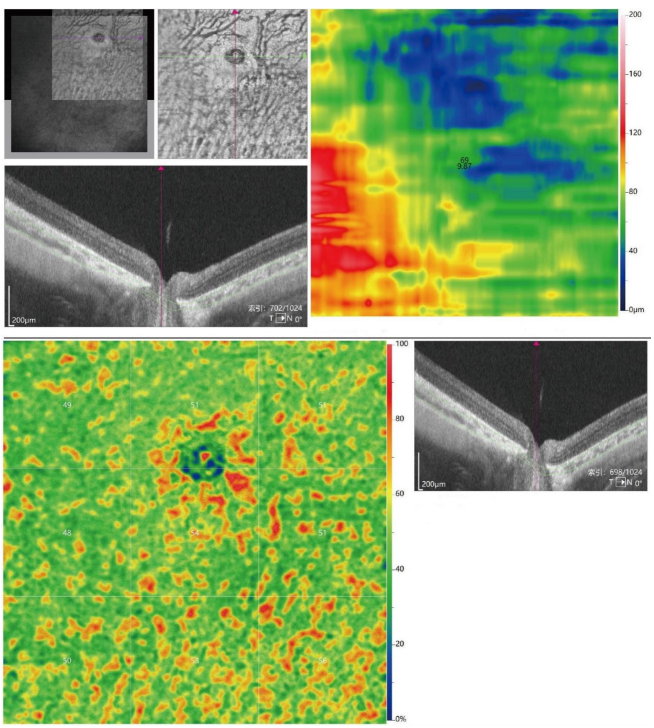

Figure 1 Choroidal thickness and vascular density in the control group of guinea pigs.

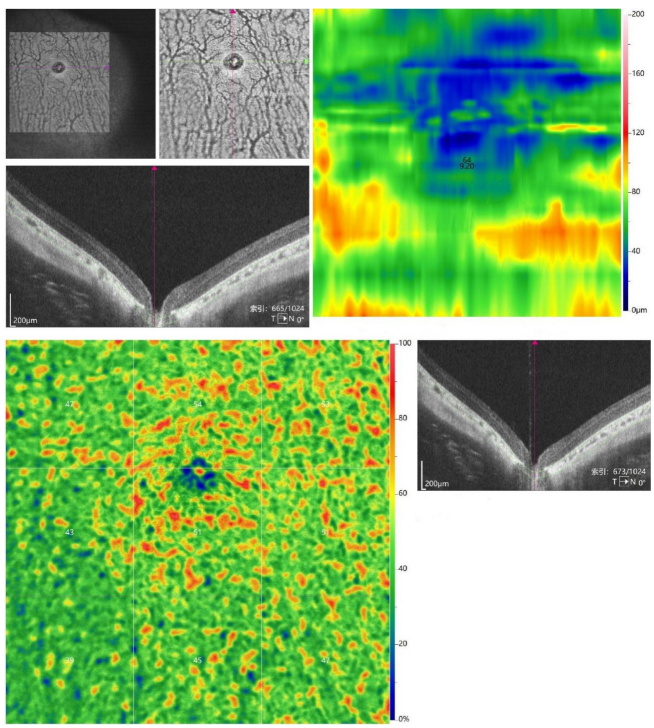

Figure 2 Choroidal thickness and vascular density in the form deprivation myopia group of guinea pigs.

the feasibility of our modeling method. After EA treatment, the myopic refractive error in the EA group significantly decreased, indicating that EA effectively reduces myopic refractive error and improves refractive status.

Following successful myopia modeling, the choroidal vascular density of guinea pigs in the FDM group, FDM+EA group, and FDM+sham acupuncture group significantly decreased, indicating that myopia reduces choroidal vascular density and blood perfusion. The specific mechanism may involve local hypoxia in the choroidal tissue due to myopia, which further leads to decreased vascular density and reduced blood perfusion in the choroid. This warrants further investigation.

After EA treatment, the choroidal vascular density in the FDM+EA group significantly increased, while no significant increase was observed in the FDM+sham acupuncture group. This suggests that EA treatment may improve the pathological state of myopia by increasing choroidal blood perfusion. After EA treatment, the mRNA levels of PI3K, Akt, mTOR, and

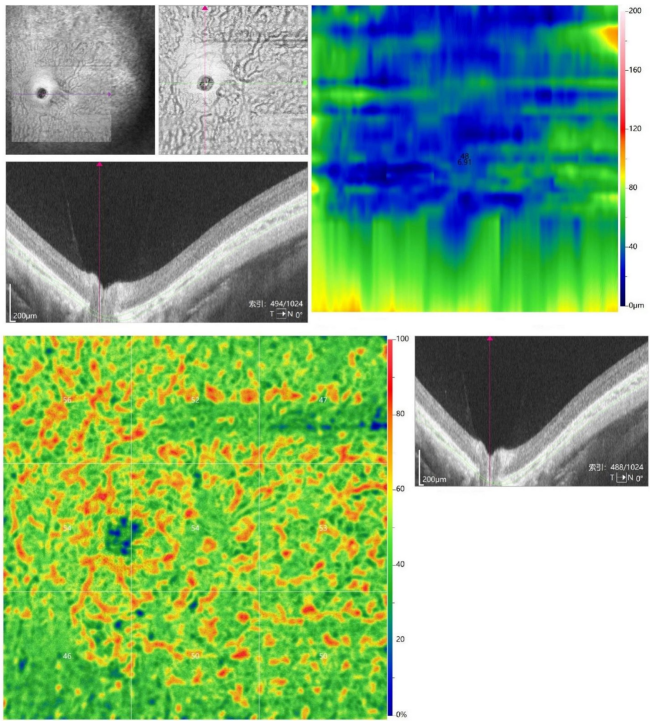

Figure 3 Choroidal thickness and vascular density in the electroacupuncture group of guinea pigs.

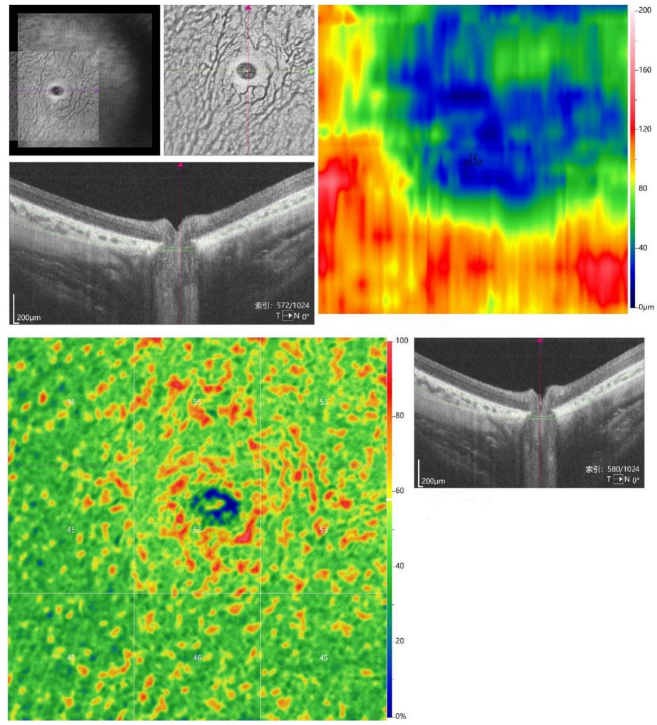

Figure 4 Choroidal thickness and vascular density in the sham acupoint group of guinea pigs.

Table 4 Analysis of relative gene expression levels across experimental groups $\bar{x}\pm s$

Groups	PI3K	Akt1	mTOR	HIF-1α
Control group ($n=8$)	1.024±0.173	1.021±0.177	1.006±0.181	1.026±0.272
FDM group ($n=8$)	1.801±0.212[a]	2.095±0.194[a]	2.246±0.141[a]	2.427±0.328[a]
FDM+EA group ($n=8$)	1.378±0.218[a,b]	1.473±0.192[a,b]	1.512±0.212[a,b]	1.518±0.232[a,b]
FDM+sham group ($n=8$)	1.725±0.242[a]	1.982±0.183[a]	2.139±0.118[a]	2.314±0.303[a]

EA: Electroacupuncture; FDM: Form deprivation myopia; PI3K: Phosphatidylinositol 3-kinase; Akt1: AKT serine/threonine kinase 1; mTOR: Mammalian target of rapamycin; HIF-1α: Hypoxia-inducible factor 1-alpha. [a]Significantly different from the control group; [b]Significantly different from the FDM group.

HIF-1α in the FDM+EA group significantly decreased compared to the FDM group.

The pathogenesis of myopia is primarily attributed to active scleral remodeling, with numerous studies suggesting that hypoxia actsas a key regulator of extracellular matrix (ECM) remodeling in scleral cells during the development of myopia. The compensatory responses induced by myopia can thin the choroid and reduce choroidal blood perfusion. This reduction in choroidal perfusion may lead to hypoxia in the adjacent scleral tissue, thereby promoting the onset and progression of myopia. Consequently, scleral hypoxia may result from decreased choroidal blood perfusion[12].

The regulatory response induced by myopia can thin the choroidand reduce choroidal blood perfusion, which in turn may lead to hypoxia in adjacent scleral tissues. Recent studies have shown that during myopia development, scleral hypoxia induced HIF-αexpression increased and contributes to the onset and progression of myopia[13]. HIF-α is involved in cellular responses to hypoxia[14]. The mechanisms underlying myopia are highly complex. Wu *et al*[15] found that scleral hypoxia serves as a trigger for myopia. Studies have confirmed that scleral HIF-1α is an important regulatory candidate in the interplay between genetic and environmental factors underlying human myopia.

Hypoxia-induced upregulation of HIF-1α activating downstream key pathways for vascular endothelial cell proliferation, such as the PI3K/Akt/mTOR signaling pathway[16]. These findings highlight the critical role of hypoxia in scleral ECM remodeling and myopia development, thereby suggesting a potential therapeutic approach to control myopia by improving hypoxia[17]. In the future, our research group will further study the effect of EA on the proliferation of scleral fibroblasts and its mechanism.

Studies have shown that activation of the PI3K/Akt pathway plays an important role in the expression and activation of HIF-1α under hypoxicconditions[18]. HIF-1α also plays a crucial regulatory role in the pathological processes of ischemia and hypoxia in other organs. Research has confirmed that HIF-1α is a hypoxia-inducible nuclear transcription regulator, controlled by intracellular oxygen levels. During

cerebral ischemia and hypoxia, HIF-1α expression is upregulated and can induce the expression of downstream target genes[19]. Similarly, HIF-1α plays an important role in hypoxic-ischemic brain injury[20].

In traditional Chinese medicine (TCM), myopia is referred to as "near-sightedness and far-sightedness weakness". Myopia can be treated by unblocking meridians and regulating the circulation of qi and blood[21]. Studies have confirmed[22-23] that acupuncture can improve uncorrected visual acuity, with a total treatment efficacy rate of 97.9%. Research has also shown that acupuncture has a certain therapeutic effect on anisometropic amblyopia, possibly through its influence on choroidal blood perfusion in the eye.

Our prior research found that acupuncture treatment improved lens thickness, spherical equivalent refraction, and ciliary body thickness in myopia patients to some extent[6]. Studies have also demonstrated that acupuncture can improve the disease activity index in mice with ulcerative colitis, possibly by downregulating the expression of signal transducer and activator of transcription 3 (STAT3) and HIF-1α proteins in the colon and improving hypoxic conditions[24]. Acupuncture at Zusanli (ST36) and Quchi (LI11) points exerts neuroprotective effects on ischemia-reperfusion injury in the brain by regulating the PI3K/Akt signaling pathway[25].

These results suggest that EA treatment negatively regulates the expression of PI3K/Akt/mTOR-HIF-1α signaling pathway mRNA. It may further reduce HIF-1α expression by modulating the PI3K/Akt/mTOR pathway, thereby improving the hypoxic state of the sclera and inhibiting the progression of myopia. However, guinea pigs lack a macula and have a uniform choroidal capillary layer, limiting direct translation to human myopia.

Taiyang acupoint is an extra-meridian acupoint, located between the eyebrow tip and the outer canthus of the eye, about a horizontal finger or 1 inch of depression. It is located at the intersection of the Hand-Foot Shaoyang meridian, the Hand-Sun and the Hand-Yangming meridian[26]. Taiyang acupoint itself has the effect of improving vision for the eyes, because it stimulates the surrounding nerves and blood vessels, improves the blood supply state of the eyes, thereby improving vision[27]. As a sham acupoint control group, 0.5 cm above the Taiyang acupoint usually does not have a direct therapeutic effect on the eyes, but may produce non-specific reactions, such as placebo effect[28]. The acupoint is an irregular complex three-dimensional spatial structure with a certain breadth and depth, rather than an independent point or line[29]. Therefore, the area of the Taiyang point area should be more than 0.5 cm, and may be larger. In acupuncture clinical trials, the sham point control group was used to exclude the non-specificity of acupuncture, so as to more clearly observe and evaluate the specific therapeutic effect of acupuncture[30]. As an extra-meridian acupoint, Taiyang acupoint has a certain specific effect, while the sham acupoint control group is used to compare the specific and non-specific effects of acupuncture. By comparing the reaction of the sun point group and the sham point group, the specific mechanism of acupuncture can be further explored[29]. In summary, the 0.5 cm above the Taiyang point as a sham point control group is an active non-specific intervention measure to exclude the non-specific effects of acupuncture, so as to more clearly evaluate the specific therapeutic effect of acupuncture.

The core hypothesis of this study, the molecular analysis of the PI3K/Akt/mTOR-HIF-1 α signaling pathway, was only based on a small sample size, which may affect the statistical validity and universality of the research results. Due to protein expression being a more direct indicator of cellular activity, in order to fully support the proposed mechanism, our research group will further analyze the molecular mechanism of this pathway at the protein level in the future, aiming to study this pathway from a more microscopic and precise perspective.

The physiological and pathological processes in organisms may be different between males and females. Using only male animals for experiments, the results may only reflect the situation of male individuals, and cannot fully cover the physiological responses of female animals, thus limiting the extrapolation of experimental results to a wider range of animal populations and even humans. The reproductive cycle of female animals can lead to periodic changes in hormone levels in the body, which may affect the experimental results[31].

In this study, we did not analyze the expression of PI3K/Akt/mTOR-HIF-1α signaling pathway mRNA at the time points before modeling and after modeling. Thus, we could not observe time-dependent differences in the expression of each factor, which limits comprehensive analysis. This limitation will be addressed in future experiments.

In the future, our research team will conduct more in-depth and detailed mechanistic studies on how EA intervention improves scleral hypoxia and increases choroidal blood perfusion in myopia.

Conflicts of Interests: Qin H, None; Zhao Y, None; Liu M, None; Wang Y, None; Zhou S, None; Ma DC, None; Gao YX, None.

Authors' Contributions: Qin H led Zhao Y and Ma DC to conduct research, participated in data collection, and drafted the manuscript. Gao YX and Zhao Y conducted statistical analysis and participated in the design. Qin H, Wang Y, and Liu M participated in the collection, analysis, or interpretation of data and drafted the manuscript. All authors have read and approved the final manuscript.

REFERENCES

[1] Saxena R, Dhiman R, Gupta V, et al. Prevention and management of childhood progressive myopia: national consensus guidelines. Indian J Ophthalmol, 2023,71(7):2873-2881.

[2] Liang JH, Pu YQ, Chen JQ, et al. Global prevalence, trend and projection of myopia in children and adolescents from 1990 to 2050: a comprehensive systematic review and meta-analysis. Br J Ophthalmol, 2025,109(3):362-371.
[3] Qin H, Mu JY, Gao YX, et al. Epidemiological study of refractive errors among primary and middle school students in Ili, Xinjiang. Modern Medicine, 2022;50(12):1532-1535.
[4] Shah R, Vlasak N, Evans BJW. High myopia:reviews of myopia control strategies and myopia complications. Ophthalmic Physiol Opt, 2024,44(6):1248-1260.
[5] Zhang XL, Jiang JW, Kong KJ, et al. Optic neuropathy in high myopia:glaucoma or high myopia or both? Prog Retin Eye Res, 2024, 99:101246.
[6] Khanal S, Tomiyama ES, Harrington SC. Childhood myopia part I: contemporary treatment options. Invest Ophthalmol Vis Sci, 2025, 66(7):6.
[7] Pan CW, Dong XX, Lanca C, et al. Global perspectives on myopia and pathologic myopia: from environmental drivers to precision medicine. Prog Retin Eye Res, 2025,109:101415.
[8] Wang Y, Zhang YN, Gao YX. Randomized controlled trials of acupuncture for adolescents with mild-to-moderate myopia. Chinese Journal of Traditional Chinese Ophthalmology, 2015;4:231-235.
[9] Gao YX, Qin H, Wang Y, et al. Effects of electroacupuncture,EGF and EGFR on scleral remodeling in form deprivation myopia rats. Guiding Journal of Traditional Chinese Medicine and Pharmacy, 2023;29(7): 29-34, 40.
[10] Cross AJ, Thomas D, Liang J, et al. Educational interventions for health professionals managing chronic obstructive pulmonary disease in primary care. Cochrane Database Syst Rev, 2022,5(5):CD012652.
[11] Percie du Sert N, Ahluwalia A, Alam S, et al. Reporting animal research: explanation and elaboration for the ARRIVE guidelines 2.0. PLoS Biol, 2020,18(7):e3000411.
[12] Zhou X, Zhang S, Yang F, et al. Decreased choroidal blood perfusion induces myopia in guinea pigs. Invest Ophthalmol Vis Sci, 2021,62(15):30.
[13] Wu WJ, Su YC, Hu CX, et al. Hypoxia-induced scleral HIF-2α upregulation contributes to rises in MMP-2 expression and myopia development in mice. Invest Ophthalmol Vis Sci, 2022,63(8):2.
[14] Semenza GL. Regulation of erythropoiesis by the hypoxia-inducible factor pathway: effects of genetic and pharmacological perturbations. Annu Rev Med, 2023,74:307-319.
[15] Wu H, Chen W, Zhao F, et al. Scleral hypoxia is a target for myopia control. Proc Natl Acad Sci U S A, 2018, 115(30): E7091-E7100.
[16] Zhang JC, Liu QM, Hu XQ, et al. Apelin/APJ signaling promotes hypoxia-induced proliferation of endothelial progenitor cells *via* phosphoinositide-3 kinase/Akt signaling. Mol Med Rep, 2015,12(3): 3829-3834.
[17] Lam DS, Zhao JH, Chen LJ, et al. Adjunctive effect of acupuncture to refractive correction on anisometropic amblyopia: one-year results of a randomized crossover trial. Ophthalmology, 2011, 118(8):1501-1511.
[18] Zhao JH, Lam DS, Chen LJ, et al. Randomized controlled trial of patching vs acupuncture for anisometropic amblyopia in children aged 7 to 12 years. Arch Ophthalmol, 2010,128(12):1510-1517.
[19] Singh N, Sharma G, Mishra V, et al. Hypoxia inducible factor-1: its potential role in cerebral ischemia. Cell Mol Neurobiol, 2012,32(4): 491-507.
[20] Barteczek P, Li LX, Ernst AS, et al. Neuronal HIF-1α and HIF-2α deficiency improves neuronal survival and sensorimotor function in the early acute phase after ischemic stroke. J Cereb Blood Flow Metab, 2017,37(1):291-306.
[21] Fanrong L, Jiping Z. Acupuncture science. Beijing: People's Medical Publishing House 2014:338.
[22] Bai TT. Mechanism of epidermal growth factor promoting the proliferation of human follicle dermal papilla stem cells. Jilin University, 2016.
[23] Wang M. Study on the effects of ulinastatin on the p38MAPK signaling pathway in rats with acute kidney injury. Shanxi Medical University, 2016.
[24] Lin SR, Zhang HJ, Wu QF. Effect of acupuncture and moxibustion on expression of signal transducers and activators of transcription 3 and hypoxia-inducible factor 1α in colon mucosa in ulcerative colitis mice. Acupunct Res, 2020,45(9):696-701.
[25] Xue XH, You YM, Tao J, et al. Electro-acupuncture at points of Zusanli and Quchi exerts anti-apoptotic effect through the modulation of PI3K/Akt signaling pathway. Neurosci Lett, 2014,558:14-19.
[26] Si ZH, Zhou YB, Yang YJ, et al. The name, location and needling method of Taiyang point. Global Chinese Medicine, 2024, 17(8):1585-1588.
[27] Jing F. Study on the effect of "Guoyanre" acupuncture on the apoptosis of retinal ganglion cells and the expression of Bax and Bcl-2 in rats with non-arteritic anterior ischemic optic neuropath. Gansu University of Traditional Chinese Medicine, 2023.
[28] Gao B, Song JK, Bi HS. Choosing acupoint in acupuncture treatment for myopia and evaluation. Technology Vision, 2020, 10: 186-188.
[29] Liu LY, Wei W, Tian J, et al. Discussion on the setting of sham acupuncture control in randomized controlled trials of acupuncture assisted reproduction. Journal of Chengdu University of Traditional Chinese Medicine, 2020,43(04):72-76.
[30] Jiang TF, Guo J. Research summary of brain functional magnetic resonance imaging with acupoint specificity. Chinese Journal of Traditional Chinese Medicine, 2021,36(8):4820-4823.
[31] Xu M, Shen YM, Han XY, et al. "One stone and two birds" strategy to treat neovascular age-related macular degeneration by a novel retinoid drug, EYE-101. Exp Eye Res, 2023,227:109385.